High-Sensitivity Hydrogen Detection With Tantalum Metal Hydride-Coated Tilted Fiber Bragg Gratings

Kasun Prabuddha Dissanayake, Ziqing Yuan, Herman Schreuders, Théo Travers, Lars J. Bannenberg, and Roger M. Groves

***Abstract*—This article presents the development and characterization of a tilted fiber Bragg grating (TFBG) hydrogen sensor functionalised with a nanometre-scale multilayer thin film stack comprising tantalum (Ta), palladium-gold ($Pd_{0.6}Au_{0.4}$), and polytetrafluoroethylene (PTFE). Ta is introduced as a novel optical fiber sensing material for hydrogen detection, offering unique advantages in sensitivity, reversibility, and hysteresis-free behavior. The optical design of the TFBG ensures efficient coupling to cladding modes, enabling a stable and repeatable hydrogen-induced spectral response when coated with Ta. The sensor was tested over a wide hydrogen concentration range from 0.001% to 100% H_2 at room temperature. Experimental results demonstrate a measurable and reversible optical response in the mean center wavelength of the cladding mode resonances, averaged over the 1520–1580-nm spectral envelope, with a minimum detection limit of 0.001% (~10 ppm) H_2 and a maximum mean wavelength shift of approximately 15 pm at 100% H_2. The Ta coating provides excellent optical performance, characterized by an absence of hysteresis and a large, nearly constant relative sensitivity across an exceptionally wide sensing range spanning at least five orders of magnitude in hydrogen concentration. Sensor stability and repeatability were further confirmed through extended cycling between 0.1% and 4% H_2, validating the robustness of the cladding mode response. These results highlight both the unique TFBG-based optical architecture and the role of Ta as a high-performance coating, supporting the potential of the Ta-TFBG sensor for sensitive, low-level hydrogen detection in aerospace and energy applications.**

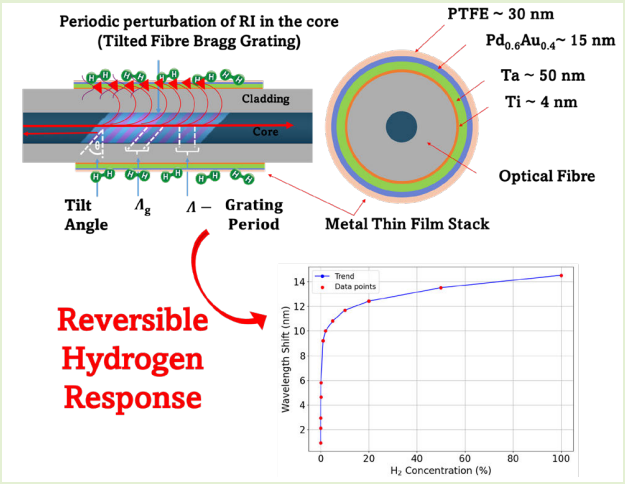

***Index Terms*— Fiber optic sensors, hydrogen sensors, metal hydrides, tantalum (Ta), tilted fiber Bragg grating (TFBG).**

I. Introduction

THE global energy sector is undergoing a transformative shift toward decarbonisation to mitigate the impacts of climate change driven by carbon dioxide (CO_2) emissions. Hydrogen has emerged as a major alternative to conventional carbon-based fossil fuels in this transition, owing to its high-gravimetric energy density and clean exhaust characteristics [1]. Its potential applications span a wide range of sectors, including energy storage, transportation, industrial processes, and aviation [2], [3], [4], where the reduction of greenhouse gas emissions is a critical objective. However, the safe and effective use of hydrogen requires advanced sensing technologies capable of accurately monitoring hydrogen concentrations, particularly in challenging operational environments [5], [6], as hydrogen-air mixtures containing more than 4% hydrogen are highly flammable [7].

Fiber-optic-based sensors offer distinct advantages under such demanding conditions due to their small size, negligible sensitivity to electromagnetic interference, spark-free operation, robustness [8], and capability for remote and distributed sensing even with submillimeter spatial resolution [9]. Among

Received 14 February 2026; revised 18 April 2026; accepted 30 April 2026. Date of publication 15 May 2026; date of current version 2 July 2026. This work was supported in part by the Clean Aviation Joint Undertaking and its members, in part by European Union Clean Aviation Project Hydrogen Demonstrator for Aviation (HYDEA) under Project 101102019, and in part by the Horizon Europe Project nOVel low-prEssure cRyogenic Liquid hydrogEn storAge For aviation (OVERLEAF) under Project 101056818. The associate editor coordinating the review of this article and approving it for publication was Dr. Juan A. Lenero-Bardallo. *(Corresponding author: Kasun Prabuddha Dissanayake.)*

Kasun Prabuddha Dissanayake, Théo Travers, and Roger M. Groves are with the Department of Aerospace Structures and Materials, Faculty of Aerospace Engineering, Delft University of Technology, 2629 HS Delft, The Netherlands (e-mail: k.p.w.dissanayake@tudelft.nl).

Ziqing Yuan, Herman Schreuders, and Lars J. Bannenberg are with the Faculty of Applied Sciences, Delft University of Technology, 2629 HS Delft, The Netherlands.

Digital Object Identifier 10.1109/JSEN.2026.3691927

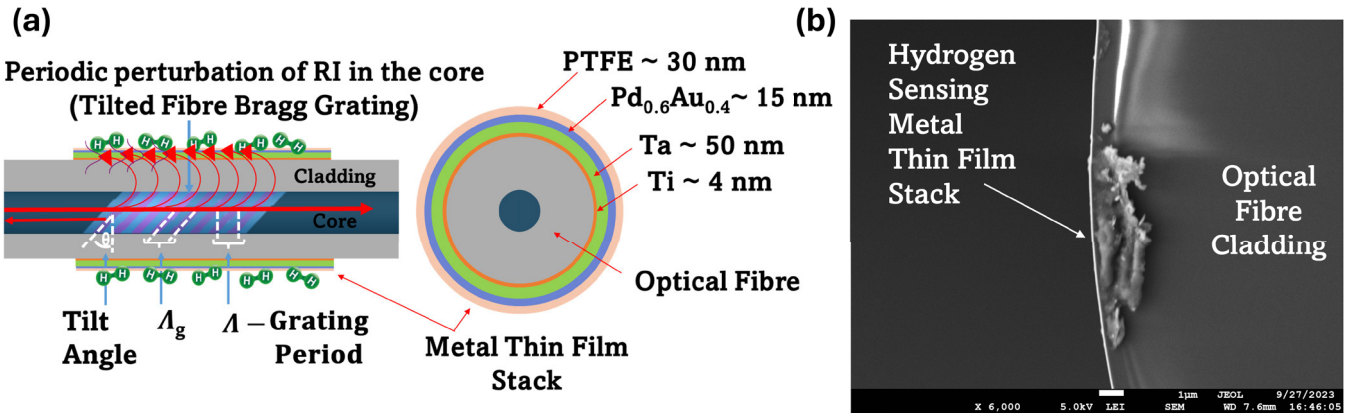

Fig. 1. (a) Schematic of the Ta-TFBG hydrogen sensor design, highlighting the hydrogen-sensitive metal thin film stack (not to scale). (b) Zoomed cross-sectional SEM image highlighting the nanometre-thick metal thin film stack on the fiber surface (low-energy electron imaging (LEI) mode).

the various fiber optic sensor configurations explored for hydrogen detection so far, including intensity-based micromirror sensors [10], surface plasmon resonance sensors [11], and interferometer-based hydrogen sensors [12], [13], [14], fiber-grating-based sensors have emerged as promising candidates due to their ease of fabrication, temperature compensation capability, and multipoint operation [15]. Within this category, tilted fiber Bragg gratings (TFBGs) are of particular interest [16], [17], [18], [19], as they exhibit strong sensitivity to changes in the external refractive index (RI), making them highly suitable for gas sensing applications.

Metal hydrides, particularly palladium (Pd), have been extensively studied as sensing materials for optical hydrogen detection. While Pd-based hydrogen sensors have demonstrated promising performance [18], [20], challenges, such as limited sensing range, hysteresis caused by phase transitions at higher hydrogen concentrations, and coating delamination have been reported [21], [22], highlighting the need for alternative materials. To address these limitations, tantalum (Ta) has recently been introduced as a potential hydrogen sensing material due to its high sensitivity, fast (subsecond) response times, high-hydrogen solubility, hysteresis-free behavior across a full hydrogen concentration range from ppm up to 100%, wide operating temperature range, and the ability to tune its sensing characteristics by alloying it with other metals such as Pd or ruthenium, depending on the specific application [23], [24], [25], [26], [27]. While Pd-coated sensors exhibit larger wavelength shifts compared to Ta, the practical advantages of Ta mentioned above outweigh this limitation.

In this work, a novel fiber optic hydrogen sensor has been developed by combining a Ta metal hydride coating with a TFBG optical transducer, leveraging the advantages of both components. The sensing principle, experimental setup, and sensor response to varying hydrogen concentrations are discussed in detail. The developed Ta-coated TFBG (Ta-TFBG) was exposed to hydrogen concentrations ranging from 10 ppm (0.001%) to 100% at room temperature (23 °C) to evaluate its performance. This concentration range encompasses the lower flammability limit of hydrogen in air (approximately 4%), making the sensor highly suitable for early stage hydrogen leak detection. Unlike many previously reported Pd-based TFBG hydrogen sensors [16], [17], [19], which rely on amplitude shifts, the proposed Ta-based sensor provides a wavelength shift response, offering a more robust and drift-resistant sensing metric. The results demonstrate the significant potential of Ta-coated TFBGs as reliable, highly sensitive hydrogen sensors for leak detection and other safety-critical applications.

II. Hydrogen Sensing Thin Film Stack and Sensing Principle

As illustrated in Fig. 1, the Ta-TFBG sensor design features a hydrogen-sensitive thin film stack composed of a 4-nm titanium (Ti) adhesion layer, a 50-nm Ta sensing layer, a 15-nm $Pd_{0.6}Au_{0.4}$ capping layer, and a 30-nm polytetrafluoroethylene (PTFE) protective coating. The Ti layer ensures strong adhesion of the Ta film to the fiber cladding, while the Ta layer serves as the primary hydrogen-sensitive material due to its ability to gradually absorb hydrogen. This hydrogen absorption process relies on the dissociation of molecular hydrogen into atomic hydrogen, a step facilitated by the $Pd_{0.6}Au_{0.4}$ capping layer, which also protects the Ta from oxidation [28]. The outer PTFE layer serves as a barrier against humidity due to its hydrophobic nature, and mitigates interference from contaminant gases such as CO_2 and nitrogen oxides. In addition, PTFE has been shown to enhance hydrogenation kinetics by lowering of the activation energy of the hydrogen dissociation reaction and by keeping the surface clean such that more sides remain available for hydrogen dissociation [29].

The thicknesses of these layers were chosen to strike a balance between sensitivity and signal quality. In particular, the high-RI metal films—Ta and $Pd_{0.6}Au_{0.4}$—need to be carefully controlled in thickness. If they become too thick, they absorb too much of the evanescent light from the TFBG's cladding modes, causing the characteristic resonances to weaken or even disappear, thereby degrading the sensor's sensitivity and signal clarity. Conversely, excessively thin layers significantly reduce the hydrogen sensitivity of the device. Accordingly, the selected layer thicknesses were optimized based on both the present experimental study and our previous investigations reported in [23], [24], [25], [26], and [27]. Maintaining the metal layers at these optimized thicknesses preserves the

visibility of the cladding resonances while ensuring effective hydrogen sensing through absorption in the sensing layer.

Metal hydrides are compounds formed when a host metal (M) absorbs hydrogen (H) upon exposure to a hydrogen-containing environment. The sensing principle relies on hydrogen absorption by the metallic layer ($M + xH \rightarrow MH_x$). The thin-film stack reversibly absorbs hydrogen, altering its optical properties—primarily the RI (n) and extinction coefficient [28]—even at very low concentrations. The TFBG transducer converts these changes into measurable spectral variations, whose magnitude depends mainly on the complex RI of the sensing layer, n_{sensing}, which varies with hydrogen concentration. The resulting RI changes affect the coupling conditions of the cladding modes in the TFBG, producing measurable shifts in the center wavelength and amplitude of the cladding mode resonances in the transmission spectrum. By tracking these spectral changes, the surrounding hydrogen concentration can be quantitatively determined. It is worth noting that the absorption of hydrogen can be accompanied by volumetric expansion of the thin film layers, which may give rise to strain-induced perturbations in the grating period as well as strain-related variations in the RI of the grating region. These effects of hydrogen absorption can be quantified through analysis of the TFBG transmission spectrum, with changes in wavelength shift and amplitude serving as key indicators underlying the sensor's hydrogen detection mechanism.

The center wavelength of the Bragg peak of the TFBG can be expressed as follows [30]:

$$\lambda_{\text{Bragg}} = \frac{\left[n_{\text{eff}}^{\text{core}}(\lambda) + n_{\text{eff}}^{\text{core}}(\lambda)\right]\Lambda_g}{\cos\theta}. \tag{1}$$

The center wavelength of the ith cladding resonance in the TFBG transmission spectrum is defined as follows:

$$\lambda_{\text{clad},i} = \frac{\left[n_{\text{eff}}^{\text{core}}(\lambda) + n_{\text{eff,clad}}^{i}\left(\lambda, n_{\text{sensing}}\right)\right]\Lambda_g}{\cos\theta}. \tag{2}$$

The reflectivity (R) or amplitude of individual cladding mode resonances can be expressed as follows [31]:

$$R = \tanh^2\left(k\left(n_{\text{sensing}}\right)L\right) \tag{3}$$

where: $n_{\text{eff}}^{\text{core}}(\lambda)$ is the effective RI of the core mode; $n_{\text{eff,clad}}^{i}(\lambda, n_{\text{sensing}})$ is the effective RI of the ith cladding mode, dependent on the RI of the hydrogen-sensitive thin film stack; n_{sensing} is the RI of the hydrogen-sensitive thin film stack; λ is the wavelength; L is the length of the TFBG; $k(n_{\text{sensing}})$ is the coupling coefficient between the ith cladding mode and the core mode, dependent on n_{sensing}; Λ_g is the grating period (distance between two tilted grating planes); and θ is the tilt angle of the TFBG.

As n_{sensing} varies with the surrounding hydrogen concentration due to the absorption of hydrogen by the layers, both $n_{\text{eff,clad}}^{i}$ and the coupling coefficient k change, leading to measurable variations in the center wavelength and amplitude of the cladding mode resonances in the TFBG transmission spectrum. By monitoring these spectral characteristics, the hydrogen concentration in the surrounding environment can be effectively quantified.

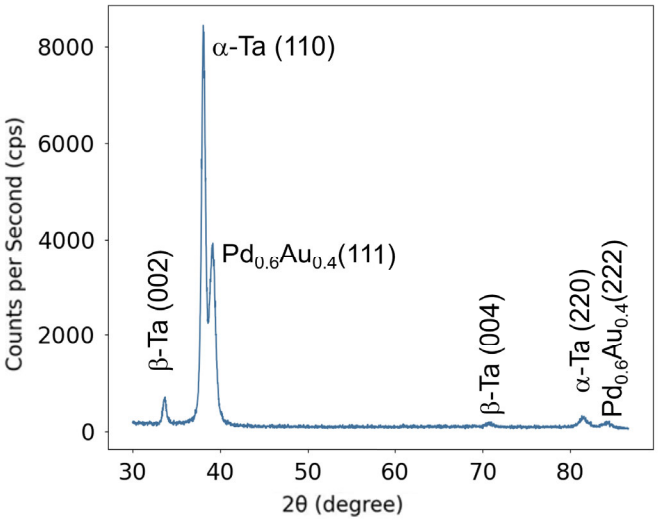

Fig. 2. XRD pattern of the hydrogen sensing metal thin film stack.

III. Sensor Fabrication

The fabrication process of the sensor involved the deposition of nanometre-thick metal thin films onto the surface of a TFBG using a magnetron sputtering technique. Prior to deposition, the fiber surface was cleaned with isopropyl alcohol to remove any contaminants. The metal thin film stack was then deposited onto the TFBG using a magnetron sputtering system (AJA Int.) with a base pressure of 10^{-6} Pa. During deposition, the fiber was mounted on a rotating holder under an argon (Ar) atmosphere maintained at 0.3 Pa to ensure uniform coating. The sputtering parameters and conditions were consistent with those reported in our previous work [23], [24], [25]. The thickness of each layer was controlled by adjusting the deposition time.

To characterize the coating, a 10 × 10 × 0.5 mm quartz substrate was placed adjacent to the fiber, allowing the same thin film stack to be deposited on both surfaces. This stack on the quartz substrate was subsequently analyzed using X-ray diffraction (XRD) and X-ray reflectivity (XRR) to evaluate the structure and thickness of the coating. Fig. 2 shows the XRD pattern of the deposited stack.

The diffraction peaks corresponding to the (111) and (222) planes confirm the presence of the $Pd_{0.6}Au_{0.4}$ capping layer. In addition, the peaks at the (110) and (220) planes of α-phase Ta [23], along with the (002) and (004) peaks of β-phase Ta [25], confirm the presence of both α and β phases of Ta in the coating. These peaks indicate the crystalline nature and phase composition of the deposited layers, confirming that the films have distinct and well-defined crystal structures.

XRR analysis revealed the layer thicknesses to be 4-nm Ti, 50-nm Ta, 15-nm $Pd_{0.6}Au_{0.4}$, and 30-nm PTFE. Based on this characterization, a uniform and well-defined thin film stack was successfully deposited on the TFBG, with the coating on the fiber expected to be similar to that on the quartz substrate, apart from minor variations.

The TFBGs used in this work were fabricated by B-Sens BV using a phase mask technique on a standard photosensitive single-mode optical fiber with a core RI of 1.45 and a cladding

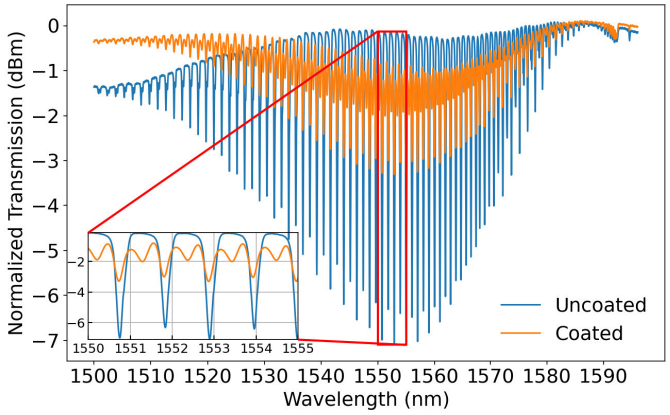

Fig. 3. Transmission spectrum of the TFBG before and after deposition of the hydrogen-sensitive metal thin film stack, recorded using unpolarized input light.

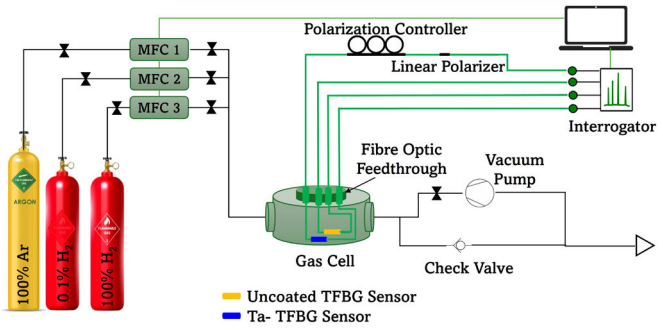

Fig. 4. Experimental setup for hydrogen sensing using the Ta-coated TFBG, including gas mixing via MFCs, a sealed chamber, and optical interrogation through the LUNA Hyperion Si155 system.

RI of 1.445. A tilt angle of 6° was selected to ensure that the cladding resonance envelope is centered around 1550 nm. The length of the TFBG was 10 mm.

Fig. 3 presents the transmission spectrum of the TFBG before and after the deposition of the metal sensing layer, recorded using unpolarised input light. As anticipated, a notable reduction in the amplitude of the cladding mode resonances is observed following the deposition, which can be attributed to the higher RI of the metal thin film stack compared to that of the fiber cladding, as measured and reported in [32] and consistent with established TFBG behavior [30]. The reduced amplitudes of the cladding mode resonances primarily arise from the lossy nature of the high-index metal coating, which introduces absorption and scattering losses that attenuate the transmitted signal.

Another important feature observed after coating is the distinct splitting of the cladding resonances relative to the uncoated TFBG spectrum. The pronounced splitting of the cladding resonances can be attributed to the optical anisotropy of the coating, which causes the HE and EH cladding modes to experience different effective refractive indices and hence distinct resonant wavelengths. This behavior is in agreement with prior studies on metal-coated TFBG sensors [30]. While such split-mode characteristics are typically prominent only in higher order modes of the TFBG spectrum, the presence of the high-RI thin film stack induces this effect across all cladding resonances. This universal mode splitting enhances the sensor's ability to resolve polarization-dependent spectral features, which is valuable for understanding vectorial sensing responses. In the present study, the polarization state yielding the highest wavelength sensitivity will be selected for further analysis, as detailed in Section IV.

IV. Experimental Setup

A leak-free gas chamber was employed to characterize the performance of the Ta-coated TFBG fiber optic hydrogen sensor across a wide range of hydrogen concentrations. The chamber was connected to three gas cylinders—pure Ar, 100% H_2, and 0.1% H_2 in Ar—through three independently controlled mass flow controllers (MFCs). These MFCs enabled precise regulation of the flow rates from each cylinder, allowing fine control over the resulting hydrogen concentration within the chamber. All experiments were conducted at room temperature. (approximately 23 °C) and under atmospheric pressure within the gas cell. Before testing, sensors were stabilized under continuous Ar flow for 2 h, followed by multiple full H_2 loading/purging cycles to eliminate initial stress artifacts and ensure repeatable responses. During measurements, total flow was maintained at 200 sccm.

The hydrogen volume fraction was calculated based on the real-time flow rate ratios, and the output from the MFCs was recorded at a 1-Hz sampling rate throughout the experiment for traceability and repeatability. The Ta-TFBG sensor was mounted securely inside the chamber in a manner that ensured the sensing region, i.e., the Ta-coated section, did not come into contact with the chamber walls to avoid mechanical interference. A reference TFBG, identical in structure but uncoated, was positioned adjacent to the sensor to monitor and compensate for any temperature- or flow-induced strain effects during measurement. Both the sensing and reference fibers were connected to a LUNA Hyperion Si155 optical interrogator (wavelength repeatability of 0.3 pm at 1 Hz and a dynamic range of 35 dB) via a hermetically sealed fiber optic feedthrough (SQS Vláknová Optika A.S.).

To further enhance the measurement accuracy, a polarization controller combined with a linear polariser was employed to control the input polarization state of the light coupled into the fiber. This setup enabled selective interrogation of the cladding resonance mode most sensitive to wavelength shifts induced by hydrogen among the previously described split polarization modes.

The transmission spectrum of the TFBG sensor was continuously monitored and recorded with a measurement interval of 5 s. The sensor response was measured for a series of hydrogen concentrations: 0.001%, 0.005%, 0.01%, 0.05%, 0.1%, 1%, 2%, 5%, 10%, 20%, 50%, and 100%. Each hydrogen concentration step was held constant for a duration of 1 h. A complete loading and unloading cycle was performed across the entire concentration range from 10 ppm to 100% H_2. As mentioned previously, hydrogen concentrations are reported as volume percentages, calculated based on the flow rates from the MFCs. Fig. 4 illustrates the experimental setup used for these measurements.

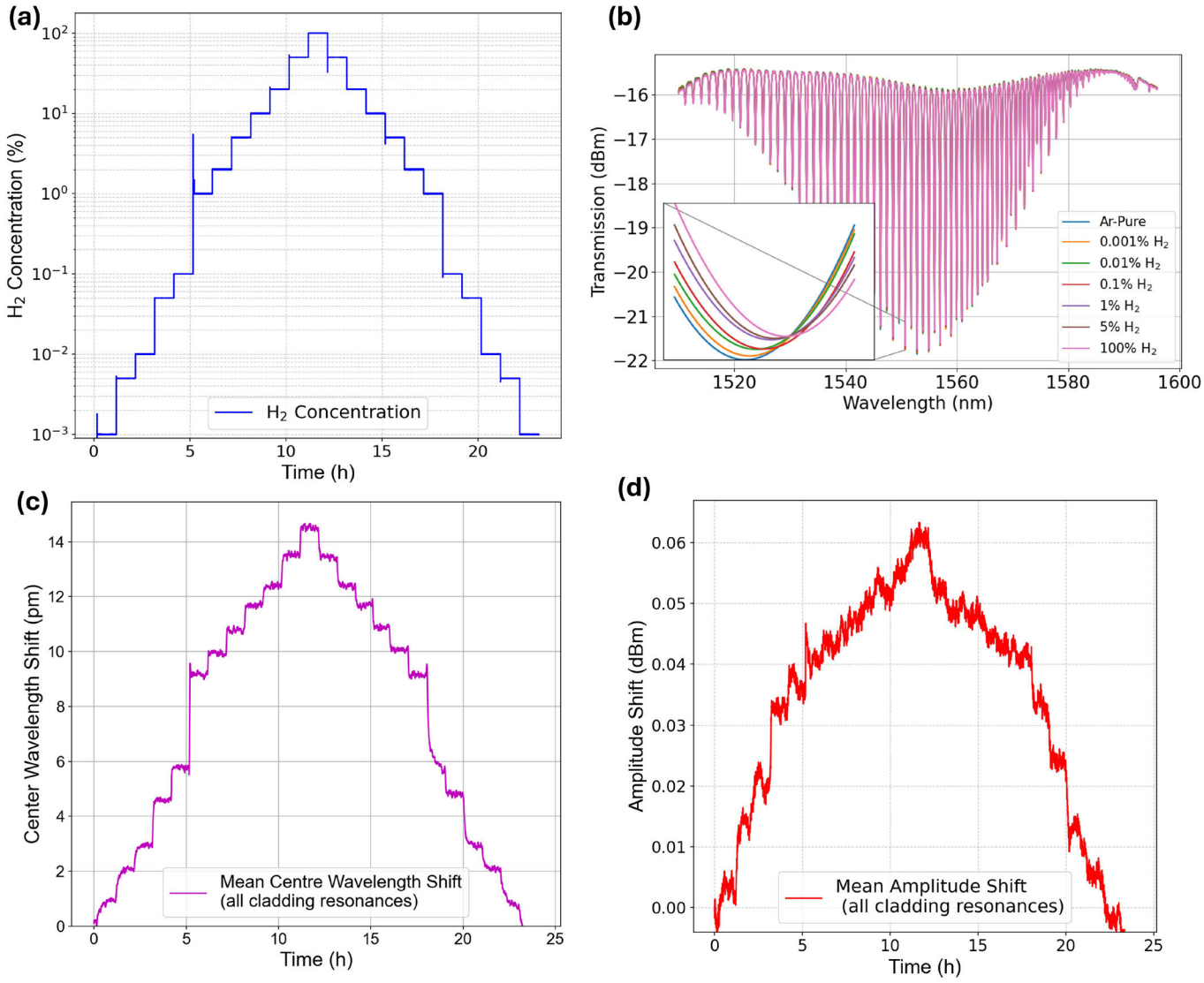

Fig. 5. Time-resolved response of the Ta-coated TFBG sensor under a full-hydrogen exposure cycle ranging from 0.001% to 100% H_2. (a) Applied H_2 concentration profile calculated from the actual values recorded by the MFCs. (b) Transmission spectrum of the Ta-TFBG under different hydrogen concentrations recorded under polarized input illumination and used to isolate a single cladding-mode branch from the polarization-induced splitting. (c) Mean wavelength shift of cladding resonances between 1520 and 1580 nm. (d) Mean amplitude shift cladding resonances between 1520 and 1580 nm. The sensor demonstrates reversible and stable wavelength shifts to dynamic H_2 variations.

V. Results and Discussion

A. Dynamic Hydrogen Response of the Ta-TFBG Sensor

The sensing performance of the Ta-coated TFBG sensor was evaluated under a full hydrogen concentration cycle ranging from 0.001% to 100% and back to 0.001%. The hydrogen concentration was varied in discrete steps during both the loading and unloading phases, providing a complete hydrogenation and dehydrogenation cycle for performance assessment.

The time-resolved dynamic response of the sensor is shown in Fig. 5, which includes the applied hydrogen concentration profile (a), Transmission spectrum of the Ta-TFBG under different hydrogen concentrations (b), the mean center wavelength shift (c), and the mean amplitude shift (d) of the cladding resonances envelope within the 1520–1580 nm range. This range encompasses all prominent cladding mode resonances, while the ghost and Bragg modes lie outside the chosen range and are weak and not prominent in the transmission spectrum due to the tilt angle selected to maximize the strength and visibility of the cladding resonances.

The transmission spectra recorded at some of the main hydrogen concentration steps are presented in Fig. 5(b). The inset highlights a zoomed-in spectral region near 1550 nm, where a distinct and progressive red shift in the center wavelength of the cladding mode resonances is clearly observed as the hydrogen concentration increases. This wavelength shift is attributed to changes in the Ta-based sensing metal layer stack, arising from hydrogen absorption and subsequent metal hydride formation, which modify the boundary conditions of the guided cladding modes through changes in the RI. Importantly, the cladding resonances remain sharp and well-defined throughout the entire measurement range, indicating that the multilayer thin-film coating does not introduce significant

optical scattering or degrade the spectral resolution of the sensor.

As illustrated in Fig. 5(c), the mean center wavelength, calculated as the average over all cladding resonances, exhibits a continuous and monotonic red shift with increasing hydrogen concentration, followed by a near-symmetric return during unloading. A measurable and repeatable spectral shift is observed even at the lowest concentration tested, 0.001% H_2, confirming the sensor's ultralow detection limit. This capability to reliably detect hydrogen at concentrations well below the 4% lower flammability limit is particularly critical for high-risk environments such as hydrogen-powered aviation. The total mean wavelength shift across the full range exceeds 15 pm and demonstrates excellent repeatability, with minimal offset between the loading and unloading trajectories, indicating a fully reversible and hysteresis-free optical response. Minor fluctuations or sharp peaks observed in the signal are attributed to flow variations or transient spikes from the MFCs, which momentarily affect the actual hydrogen concentration in the chamber. These peaks serve as clear indicators of the material's fast dynamic response to changes in hydrogen concentration.

Fig. 5(d) presents the corresponding amplitude response of the cladding resonances. Although inherently more susceptible to noise than the wavelength shift, the amplitude variation follows a similar trend: increasing with hydrogen exposure and decreasing upon evacuation. The relatively low-signal amplitude associated with this measurement contributes to a lower signal-to-noise ratio (SNR), suggesting that the interrogator may be operating near the limit of its amplitude detection capability. The amplitude reaches its maximum value near 100% H_2 and returns to near-baseline levels during the unloading phase, further confirming the reversible nature of the sensor response. While the amplitude response provides an additional sensing channel, its higher sensitivity to external perturbations and low SNR mean it is best used to complement the more robust and reliable wavelength-based measurement, which remains the primary detection parameter for quantitative hydrogen sensing.

To quantify sensor performance, the mean wavelength shift of the cladding resonances was plotted against hydrogen concentration in Figs. 6 and 7. Fig. 6 shows the mean shift of the cladding mode envelope (1520–1580 nm) on a semilogarithmic scale, spanning five decades from 0.001% to 100% H_2. The response exhibits a well-defined logarithmic response with minimal deviation between hydrogenation and dehydrogenation cycles. The near-complete overlap confirms negligible hysteresis, demonstrating the stability and reversibility of the Ta sensing layer. These results are consistent with previous studies on Ta-based hydrogen sensors, where both α- and β-Ta phases showed robust, hysteresis-free behavior across a broad pressure range [23], [25]. Notably, the linearity observed in the semi-logarithmic plot indicates a constant relative sensitivity across five orders of magnitude in hydrogen concentration [with a sensitivity of 3 pm/decade(%H_2)]—a unique and highly desirable characteristic for practical sensing applications. The linear trend observed on the semilogarithmic scale further supports the unusually high-hydrogen solubility

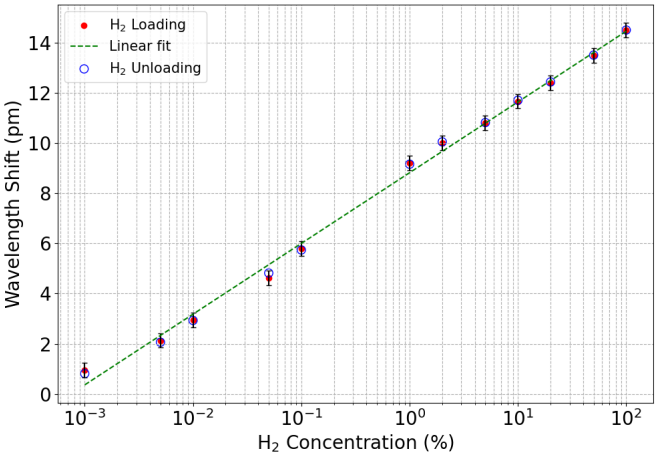

Fig. 6. Semilogarithmic plot of the mean wavelength shift of the cladding resonances as a function of hydrogen concentration from 0.001% to 100% H_2, showing a highly linear and reversible response over five orders of magnitude.

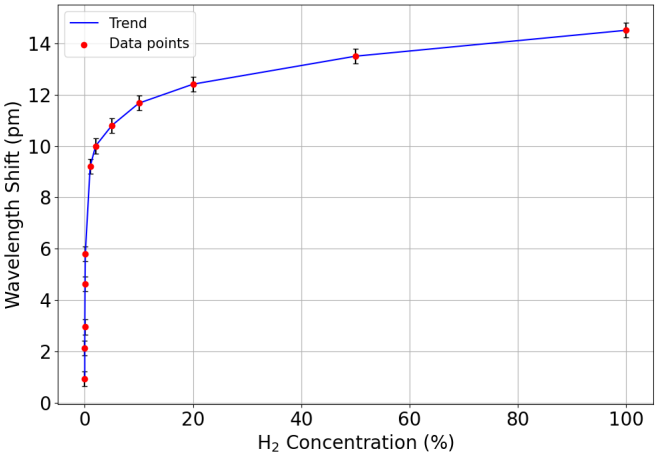

Fig. 7. Linear plot of the mean wavelength shift of the cladding resonances versus hydrogen concentration, highlighting enhanced sensitivity below 2% H_2 and the onset of saturation-like behavior at higher concentrations.

within a single crystallographic phase of Ta, thus without any phase transitions and associated hysteresis—unlike Pd-based sensors [33]. The log-linear response arises from the thermodynamics of hydrogen uptake in Ta: the metal-to-hydrogen ratio scales logarithmically with H_2 concentration [33], and since film expansion and wavelength shift both respond linearly to hydrogen uptake, the overall response is log-linear.

Fig. 7 presents the same data on a linear scale, highlighting two distinct sensitivity regimes. In the low-concentration range (0.001%–2% H_2), the sensor exhibits a steeper slope, with a sensitivity of approximately 5 pm/%H_2. This is likely due to the sharp RI changes as the Ta sensing layer absorbs relatively large amounts of hydrogen even at very low concentrations. At higher concentrations (>10% H_2), the response curve flattens slightly, indicating a modest reduction in sensitivity and a less pronounced change in signal with further increases in hydrogen concentration.

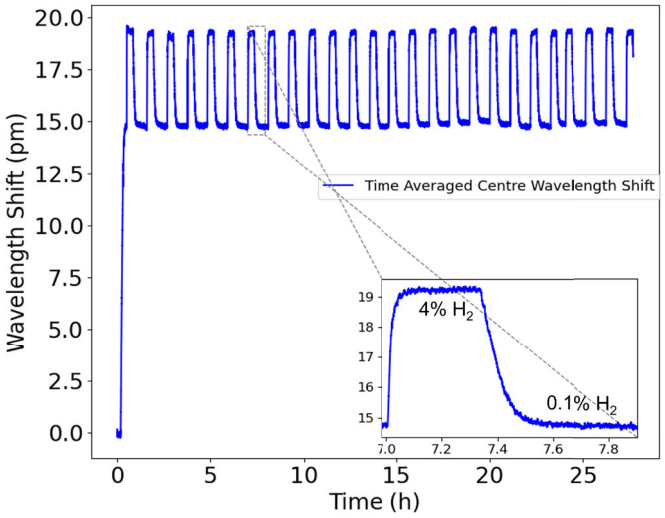

Fig. 8. Dynamic response of the Ta-coated TFBG sensor over multiple exposure cycles between 0.1% and 4% H_2. The main plot shows the wavelength shift of a representative cladding resonance centered at 1555 nm over a 28-h period, while the inset highlights a single cycle to illustrate the sensor's repeatability, fast response, and negligible hysteresis.

B. Repeatability and Stability of the Sensor

Fig. 8 presents the dynamic response of the Ta-coated TFBG hydrogen sensor subjected to repeated exposure cycles between 0.1% and 4% H_2 at room temperature. The y-axis denotes the wavelength shift of a representative cladding resonance centered at 1555 nm, chosen for its high SNR and its position within the most sensitive region of the spectrum near 1550 nm. The x-axis corresponds to the total measurement duration, which spans approximately 28 h. Each cycle is characterized by a sharp rise and fall in the center wavelength, corresponding to the alternation between high- and low-hydrogen concentrations.

The sensor exhibits a distinct, step-like, and highly repeatable spectral response across all cycles, demonstrating excellent reproducibility. Upon exposure to 4% H_2, the resonance consistently shifts by approximately 19 pm, while flushing the chamber with 0.1% H_2 leads to a return to approximately 15 pm. These abrupt and nearly symmetric transitions indicate rapid hydrogen absorption and desorption in the Ta-based metal hydride layer, highlighting the fast reaction kinetics of the sensing material.

The inset of Fig. 8 illustrates a magnified complete cycle in detail, demonstrating the sensor's ability to clearly resolve transitions between 0.1% and 4% hydrogen levels with negligible hysteresis. This segment also facilitates estimation of the sensor's temporal response. Previous work has shown that the intrinsic response time of the Ta hydrogen-sensitive material is less than 1 s when transitioning from 0.1% to 4% H_2 at room temperature [23].

In the current setup, the sensor is housed within a gas cell with an internal volume of 0.4 L. The time required for the cell to reach saturation at a given hydrogen concentration—based on the gas flow rate—must be considered when evaluating the response time. In this study, the total flow was maintained at 200 sccm. Despite the relatively large cell volume, the measured response time, defined as the duration required to reach 90% of the final wavelength shift, is approximately 100 s for hydrogenation and 500 s for recovery (dehydrogenation). We note that this represents an upper bound on the response time. The intrinsic sensor response cannot be readily extracted from these measurements because the extrinsic response of the setup is relatively large, due to the chamber's substantial volume, which leads to particularly long transients during hydrogen concentration steps.

The consistent peak wavelength shift values observed across all cycles confirm the long-term stability and robustness of the sensor. No noticeable signal drift, baseline offset, or amplitude degradation was observed over the 28-h test period, indicating minimal fatigue or performance deterioration of the sensing layer. In summary, this cycling experiment validates the durability, reversibility, and fast response of the Ta-coated TFBG sensor under repeated low- and mid-level hydrogen exposure, especially below the 4% lower flammability limit. These results confirm the sensor's suitability for continuous and repeated hydrogen monitoring, particularly in safety-critical applications where long-term reliability and repeatability are essential.

VI. Conclusion

A hydrogen sensor based on a TFBG coated with a Ta-based metal hydride multilayer thin film has been developed and experimentally validated across an extensive hydrogen concentration range from 0.001% to 100% H_2. The sensor exhibited robust and repeatable optical responses in both the amplitude and center wavelength of the cladding mode resonances, with a minimum detection limit of 0.001% H_2 and a maximum mean wavelength shift of approximately 15 pm at 100% H_2. The spectral response followed a linear trend on a semilogarithmic scale with a sensitivity of 3 pm/decade(%H_2), and negligible hysteresis was observed during full-hydrogen loading and unloading cycles, confirming the reversibility and stability of the Ta sensing layer.

Dynamic measurements revealed consistent response and recovery behavior over multiple cycles between 0.1% and 4% H_2, with response and recovery times of approximately 100 and 500 s, respectively. The sensor's wavelength-based signal exhibited low noise and high repeatability, while the amplitude response, although more susceptible to external perturbations, provided complementary information. Enhanced sensitivity was observed in the sub-2% H_2 range, indicating potential for early leak detection well below the 4% lower flammability limit in air.

These results confirm the suitability of Ta-coated TFBG sensors for low-level hydrogen detection and real-time monitoring in harsh environments. Future work will focus on extending the operational temperature range and assessing long-term reliability under thermally and mechanically dynamic conditions relevant to aerospace, energy, and hydrogen infrastructure safety. Ta has already demonstrated excellent hydrogen sensing performance at both elevated (270 °C) and cryogenic (−60 °C) temperatures [26], [27].

The optical design of the Ta-TFBG sensor may be further optimized by tuning the thicknesses of the multilayer stack to improve the response time and employing higher tilt angles to excite higher order cladding modes, thereby enhancing the wavelength sensitivity. Ongoing efforts will also aim to decouple the RI response from strain effects associated with hydride-induced expansion, by leveraging the polarization-dependent split cladding resonances introduced by the thin-film structure, as well as by tracking the Bragg (core mode) resonance to quantify and subtract temperature and strain contributions from the cladding mode shifts induced by hydrogen absorption near the fiber surface.

REFERENCES

[1] J. A. Turner, "Sustainable hydrogen production," *Science*, vol. 305, no. 5686, pp. 972–974, 2004.

[2] L. Schlapbach and A. Züttel, "Hydrogen-storage materials for mobile applications," *Nature*, vol. 414, no. 6861, pp. 353–358, 2001.

[3] I. Staffell et al., "The role of hydrogen and fuel cells in the global energy system," *Energy & Environ. Sci.*, vol. 12, no. 2, pp. 463–491, 2018.

[4] (2019). *The Future of Hydrogen: Seizing Today's Opportunities*. [Online]. Available: https://www.iea.org/reports/the-future-of-hydrogen

[5] C. Jia et al., "A review of hydrogen sensors for ECLSS: Fundamentals, recent advances, and challenges," *Appl. Sci.*, vol. 13, no. 12, p. 6869, Jun. 2023.

[6] T. Yusaf et al., "Sustainable hydrogen energy in aviation—A narrative review," *Int. J. Hydrogen Energy*, vol. 52, pp. 1026–1045, Jan. 2024.

[7] *Hydrogen Safety*. Accessed: Apr. 19, 2025. [Online]. Available: https://www1.eere.energy.gov/hydrogenandfuelcells/pdfs/h2_safety_fsheet.pdf

[8] G. Wang, J. Dai, and M. Yang, "Fiber-optic hydrogen sensors: A review," *IEEE Sensors J.*, vol. 21, no. 11, pp. 12706–12718, Jun. 2021.

[9] K. Dey et al., "High-density fiber Bragg grating array enabling fully distributed sensing with sub-millimeter spatial resolution," *Opt. Lett.*, vol. 51, no. 1, pp. 117–120, 2026.

[10] D. J. Verhoeff, H. Schreuders, and L. J. Bannenberg, "Tantalum-palladium alloy based optical micro-mirror hydrogen sensor," *Sens. Actuators B, Chem.*, vol. 428, Apr. 2025, Art. no. 137229.

[11] A. Hosoki, M. Nishiyama, H. Igawa, A. Seki, and K. Watanabe, "A hydrogen curing effect on surface plasmon resonance fiber optic hydrogen sensors using an annealed Au/Ta_2O_5/Pd multilayer film," *Opt. Exp.*, vol. 22, pp. 18556–18563, Jul. 2014.

[12] B. Du et al., "Highly sensitive hydrogen sensor based on an in-fiber Mach–Zehnder interferometer with polymer infiltration and Pt-loaded WO_3 Coating," *Opt. Exp.*, vol. 29, no. 3, pp. 4147–4158, Feb. 2021.

[13] J. Luo et al., "Fiber optic hydrogen sensor based on a Fabry–Perot interferometer with a fiber Bragg grating and a nanofilm," *Lab Chip*, vol. 21, pp. 1752–1758, Mar. 2021.

[14] F. Xu et al., "Ultrahigh sensitivity of hydrogen detection with a perforated pd film on a miniature fiber tip," *Sens. Actuators B, Chem.*, vol. 400, Feb. 2024, Art. no. 134875.

[15] X. Ping et al., "Fiber grating hydrogen sensor: Progress, challenge and prospect," *Adv. Sensor Res.*, vol. 3, no. 2, Feb. 2024, Art. no. 2300088.

[16] Y. Shan, Q. Zhang, B. Zhou, and H. Chen, "Highly sensitive hydrogen sensor based on a tilted fiber Bragg grating coated with Pd/WO_3 composite film," *Appl. Sci.*, vol. 13, no. 12, p. 6869, 2023.

[17] C. Zhang et al., "High sensitivity hydrogen sensor based on tilted fiber Bragg grating coated with PDMS/WO_3 film," *Int. J. Hydrogen Energy*, vol. 47, no. 9, pp. 6415–6420, Jan. 2022.

[18] J. Yu, Z. Wu, X. Yang, X. Han, and M. Zhao, "Tilted fiber Bragg grating sensor using chemical plating of a palladium membrane for the detection of hydrogen leakage," *Sensors*, vol. 18, no. 12, p. 4478, Dec. 2018.

[19] Z. Yang et al., "Ultrafast and reproducible fiber-optic hydrogen sensor via a tilted fiber grating with Pd/WO_3 nanocoating," *Photonic Sensors*, vol. 15, no. 2, 2025, Art. no. 250229.

[20] Y. Chen, Y. Yang, C. Liang, Y. Yao, and J. Chen, "Palladium-based optical fiber Bragg grating hydrogen sensors: A comprehensive review," *Opt. Laser Technol.*, vol. 175, Aug. 2024, Art. no. 110850.

[21] J. Li et al., "Boosting room temperature response of pd-based hydrogen sensor by constructing in situ nanoparticles," *Phys. E, Low-Dimensional Syst. Nanostruct.*, vol. 144, Oct. 2022, Art. no. 115464.

[22] B. Toksha, P. Gupta, and M. Rahaman, "Hydrogen sensing with palladium-based materials: Mechanisms, challenges, and opportunities," *Chem.-Asian J.*, vol. 19, no. 16, Aug. 2024, Art. no. 202400127.

[23] L. Bannenberg, H. Schreuders, and B. Dam, "Tantalum-palladium: Hysteresis-free optical hydrogen sensor over 7 orders of magnitude in pressure with sub-second response," *Adv. Funct. Mater.*, vol. 31, no. 16, Apr. 2021, Art. no. 2010483.

[24] L. J. Bannenberg, H. Schreuders, N. van Beugen, C. Kinane, S. Hall, and B. Dam, "Tuning the properties of thin-film TaRu for hydrogen-sensing applications," *ACS Appl. Mater. Interface*, vol. 15, no. 6, pp. 8033–8045, Feb. 2023.

[25] L. J. Bannenberg, D. J. Verhoeff, N. Jonckers Newton, M. Thijs, and H. Schreuders, "Structural and optical properties of thin film β-Ta upon exposure to hydrogen to assess its applicability as hydrogen sensing material," *ACS Appl. Nano Mater.*, vol. 7, no. 2, pp. 1757–1766, 2024.

[26] H. S. Dewi, K. P. Dissanayake, H. Schreuders, R. M. Groves, and L. J. Bannenberg, "Metal hydride hydrogen sensing materials from 28 °C to 270 °C," *Int. J. Hydrogen Energy*, vol. 84, pp. 606–614, Sep. 2024.

[27] Z. Yuan, H. Schreuders, R. Dankelman, B. Dam, and L. J. Bannenberg, "Optical hydrogen sensing materials for applications at sub-zero temperatures," *Adv. Funct. Mater.*, vol. 35, no. 23, Jun. 2025, Art. no. 2420087.

[28] L. J. Bannenberg, C. Boelsma, K. Asano, H. Schreuders, and B. Dam, "Metal hydride based optical hydrogen sensors," *J. Phys. Soc. Jpn.*, vol. 89, no. 5, May 2020, Art. no. 051003.

[29] L. J. Bannenberg, B. Boshuizen, F. A. Ardy Nugroho, and H. Schreuders, "Hydrogenation kinetics of metal hydride catalytic layers," *ACS Appl. Mater. Interface*, vol. 13, no. 44, pp. 52530–52541, Nov. 2021.

[30] J. Albert, L. Shao, and C. Caucheteur, "Tilted fiber Bragg grating sensors," *Laser & Photon. Rev.*, vol. 7, no. 1, pp. 83–108, 2012.

[31] X. Dong, H. Zhang, B. Liu, and Y. Miao, "Tilted fiber Bragg gratings: Principle and sensing applications," *Photonic Sensors*, vol. 1, no. 1, pp. 6–30, Mar. 2011.

[32] K. P. W. Dissanayake, H. S. Dewi, H. Schreuders, L. J. Bannenberg, and R. M. Groves, "Design of a metal hydride-coated tilted fibre Bragg grating-based hydrogen sensor," *Proc. SPIE*, vol. 12999, Jun. 2024, Art. no. 1299927.

[33] L. J. Bannenberg, L. Blom, K. Sakaki, K. Asano, and H. Schreuders, "Completely elastic deformation of hydrogenated ta thin films," *ACS Mater. Lett.*, vol. 5, no. 4, pp. 962–969, Apr. 2023.